ACS APPLIED ENERGY MATERIALS

www.acsaem.org

Article

High-Performance Thienothiophene and Single Wall Carbon Nanotube-Based Supercapacitor as a Free-Standing and Flexible Hybrid Energy Storage Material

Recep Isci,* Koray Bahadir Donmez, Nilgun Karatepe, and Turan Ozturk*

Cite This: *ACS Appl. Energy Mater.* 2024, 7, 1488−1494

Read Online

ACCESS | Metrics & More | Article Recommendations | Supporting Information

ABSTRACT: Long cycle life and high energy/power density are imperative for energy storage systems. Similarly, flexible and free-standing electrodes are important for supercapacitor applications. Herein, we report, for the first time, use of thienothiophene (TT) and a single-walled carbon nanotube (SWCNT)-based free-standing and flexible hybrid material (**TT-TPA-SWCNT**) as a high-performance supercapacitor. The synthesized TT derivative, **TT-TPA**, was directly attached to SWCNT through noncovalent interactions to obtain the TT-based SWCNT hybrid, **TT-TPA-SWCNT**, as a flexible film. The hybrid film was clarified by surface analysis methods of scanning electron microscopy and atomic force microscopy. **TT-TPA-SWCNT** was used as a flexible and free-standing electrode in a two-electrode system for supercapacitor and energy storage applications. It displayed a high energy storage capacity of 83.2 F g^{-1} at 5 mV s^{-1} scan rate, an excellent cyclic stability with 110% retention of its initial specific capacitance after 7000 cycles and a long power density ranged from 100 to 3000 W·kg^{-1}, demonstrating that **TT-TPA-SWCNT** is a promising hybrid nanomaterial for high-performance energy storage applications.

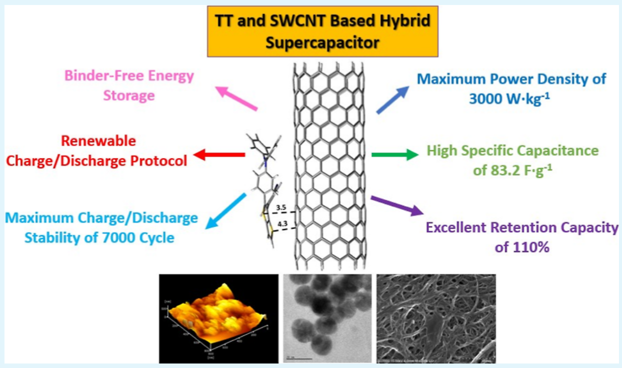

KEYWORDS: *thienothiophene, single wall carbon nanotube, supercapacitor, energy-based hybrid material, flexible and free-standing electrode*

INTRODUCTION

Energy is of great importance in the development of a human society. On the other hand, fossil fuels, nonrenewable and depleting resources, and climate-changing greenhouse gases have made our current energy system fragile.[1,2] To solve the emerging energy crisis, new generation clean energy storage and conversion technologies, fuel cells, batteries, and supercapacitors are among the most important research areas, to which scientific studies have been focused.[3] Among them, supercapacitors with fast charging/discharging rates, long cyclability, and low-cost performance have been attracting significant interest regarding their various applications including power supplies and hybrid vehicles.[4,5] Electrochemical performances of supercapacitors are mainly controlled by structural and electrochemical properties of the used materials.[6−9]

Nanocarbon materials, such as single wall carbon nanotubes (SWCNTs), have high tensile strength, good thermal conductivity, excellent resilience, porous network, and high electric conductivity, which make them suitable candidates for supercapacitor electrode applications.[10,11] Such electrodes, constructed using the SWCNT, have reached specific capacitance values of around 35 F g^{-1}.[12,13] In order to improve their electrochemical performances, SWCNT have been modified, doped, or wrapped by some inorganic and organic materials.[14,15] Although there are very limited studies, higher capacitive values have been obtained as a result of noncovalent modification of SWCNT with electron rich structures as hybrid electrodes. Moreover, noncovalent surface functionalization of SWCNT has some advantages compared to covalent modifications as the covalent modification results in a change of hybridization from sp^2 to sp^3 and partial loss of conjugation and homogeneity on the surface by some halogenation and acylation reactions.[16,17] These deformations have devastated the capacitive performance and the homogeneity of the formed electrode material for supercapacitors. Therefore, noncovalently modified SWCNT is extremely important in order to increase the energy conversion of hybrid materials, which can be obtained without losing the properties of the organic or inorganic material and the original form of

Received: October 30, 2023
Revised: January 30, 2024
Accepted: February 6, 2024
Published: February 13, 2024

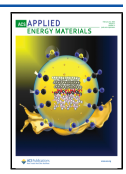

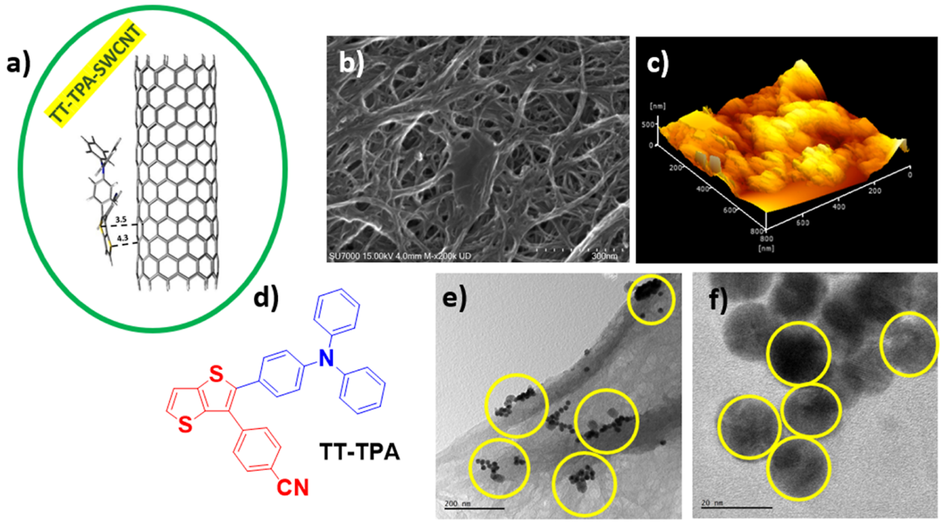

Figure 1. (a) Schematic illustration of the **TT-TPA-SWCNT** hybrid, (b) SEM image of the **TT-TPA-SWCNT** hybrid film at 200 k magnification, (c) topographical 3D AFM profile of the **TT-TPA-SWCNT** hybrid film, (d) the structure of **TT-TPA**, and TEM images of the **TT-TPA-SWCNT** hybrid treated with a gold nanoparticle solution at different magnifications: (e,f) 200 and 20 nm.

SWCNT.[18,19] Particularly, the hybrids formed by conjugated semiconductors with SWCNT have been more demanded in terms of increasing both mechanical strength and electrical conductivity.[14,15]

In particular, hybrids formed by SWCNT-conjugated semiconductors are in greater demand in terms of increasing both the mechanical strength and electrical conductivity. Well-known methods of noncovalent modifications had polymer wrapping, $\pi-\pi$ interactions, electron pull−push complexes, hydrogen bonding and van der Waals forces using π-electron or heteroatom-rich binding agents such as pyrene, porphyrin, and indole derivatives.[20,21]

Thieno[3,2-*b*]thiophene (TT) has a rigid structure with extended π-conjugation, which makes it suitable π-linker for adjusting the band gap of organic materials and to increase the intermolecular interactions in solid state.[22−26] It is an electron-rich molecule, making it a promising material for the construction of conjugated—low band gap polymeric semiconductors for energy-based applications such as organic solar cells, organic light-emitting diodes, and organic field-effect transistors.[27−36] In this report, we describe supercapacitor and energy storage performances of **TT-TPA-SWCNT** by cyclic voltammetry (CV), galvanostatic charge/discharge (GCD), and electrochemical impedance spectroscopy (EIS). For the first time, a high-performance free-standing and flexible electrode, based on a thienothiophene (TT) derivative and SWCNT, prepared without using any nonconductive binding agent, is reported. This study aimed to make an important contribution to the potential applications of TT and SWCNT-based hybrid supercapacitors for energy conversion and storage processes.

EXPERIMENTAL SECTION

Materials and Methods. All electrochemical tests were conducted using a PARSTAT MC 1000 electrochemical workstation (Amatek, USA). Free-standing and binder-free electrodes were utilized as both the working and counter electrodes. They were cut into 10 mm diameter discs and weighed before being inserted into the cell. This setup allowed a symmetrical configuration to be assembled. The experimental investigation was performed in a two-electrode system, employing an 85% H_3PO_4 electrolyte, to characterize the intrinsic electrochemical properties of **TT-TPA-SWCNT**. In a typical test, the cellulose acetate membrane was immersed into the electrolyte for 30 s before being placed into the coin cell for the electrochemical analysis. The test methods included CV, GCD, and EIS.

EIS measurements were performed over a frequency range of 100,000−0.1 Hz at an amplitude of 10 mV. To determine the suitability of the data for mathematical fitting, the Kramers−Kronig method was used for data verification. CV measurements were realized within the voltage range of 0−1 V, utilizing different scan rates of 5, 10, 20, 50, 100, 150, and 200 mV s^{-1}.

$$C_{(CV)} = \frac{2}{m(WE)k(V_2 - V_1)} \int_{V_1}^{V_2} I dV \tag{1}$$

In the given eq 1, m (WE) (g) represents the mass of the working electrode in contact with the electrolyte. The variable k denotes the scan rate used in the CV measurements. V_1 and V_2 correspond to the lowest and highest voltages, respectively, within the range employed for calculating $C_{(CV)}$.[37,38]

GCD tests were applied within the voltage range of 0.0−1.0 V at current densities of 0.20, 0.50, 1.00, 1.50, 2.00, 3.00, 4.00, and 6.00 A·g^{-1}. The gravimetric specific capacitance (C_{GCD}, F·g^{-1}), specific energy density (E, W h·kg^{-1}), and power density (P, W·kg^{-1}) of the supercapacitor were calculated from the GCD curves using the following equations.[39,40]

$$C_{GCD} = \frac{4I\Delta t}{m\Delta V} \tag{2}$$

$$E = \frac{C_{GCD}\Delta V^2}{3.6 \times 8} \tag{3}$$

$$P = \frac{3600E}{\Delta t} \tag{4}$$

In the provided 4, I (A) represents the GCD current density, Δt (s) denotes the discharge time, m (g) indicates the total mass of both electrodes, and ΔV (V) represents the discharge voltage within Δt.

RESULTS AND DISCUSSION

The hybrid electrode (**TT-TPA-SWCNT**) is composed of noncovalent modification of SWCNT with a thienothiophene derivative (**TT-TPA**) (Figure 1),[41−43] without any binding agent. In our previous study, characterization of the **TT-TPA-SWCNT** hybrid material was examined and clarified through

https://doi.org/10.1021/acsaem.3c02737
ACS Appl. Energy Mater. 2024, 7, 1488−1494

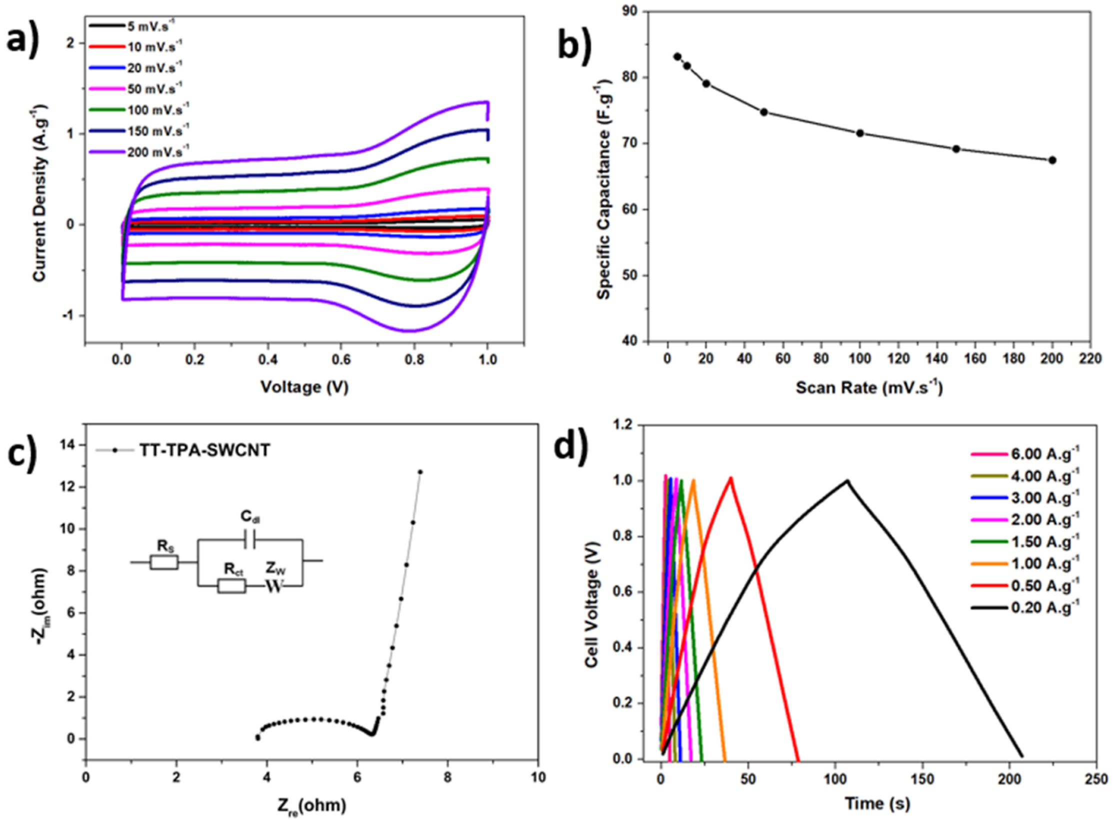

Figure 2. Electrochemical characterization of **TT-TPA-SWCNT** supercapacitor (a) CVs at different scan rates (5, 10, 20, 50, 100, 150, and 200 $mV{\cdot}s^{-1}$), (b) specific capacitances calculated from CVs at different scan rates (5, 10, 20, 50, 100, 150, and 200 $mV{\cdot}s^{-1}$), (c) Nyquist plot of the supercapacitor cell, and (d) GCD plots at various current densities (0.1, 0.25, 0.5, 0.75, 1, 1.5, 2, and 3 $A{\cdot}g^{-1}$).

both experimentally and computationally.[44] The synthesized **TT-TPA** was directly attached to SWCNT forming the **TT-TPA-SWCNT** hybrid film (Figure S1) through noncovalent interactions, i.e., van der Waals, $\pi-\pi$, and S$-\pi$, requiring no binding agents (Figure 1a). Its scanning electron microscopy (SEM) and atomic force microscopy (AFM) images showed interconnected and tangled bundles (Figure 1b) and roughness from the cross-section of the 3D AFM map (Figure 1c). In order to further clarify the surface modification of SWCNT with **TT-TPA**, the hybrid was treated with a gold nanoparticle solution, AuNPs, for Au−S interactions to obtain clear images of the nanoparticles on **TT-TPA-SWCNT** by transmission electron microscopy (TEM) at different magnifications, i.e., 200 and 20 nm (Figure 1e,f), which indicated a clear adsorption of Au by the sulfur atoms of **TT-TPAs** on the SWCNTs. This is another proof that the modification has been successfully performed on single-wall carbon nanotubes. Moreover, further photophysical properties of **TT-TPA-SWCNT** were investigated by Raman spectroscopy (Figure S2). The spectra displayed typical RBM, D, G, and 2D of SWCNT peaks at around 260, 1330, 1585, and 2650 cm^{-1}, and TT peak at around 1600 cm^{-1}. The assigned peaks proved that **TT-TPA-SWCNT** composed of TT and SWCNT cores.

CV was employed at various scan rates ranging from 5 to 200 mV s^{-1} (Figure 2a), which demonstrated that the area under the cyclic voltammograms increased with an increase in the scan rate, indicating that a supercapacitor cell possessing good rate capability. Thus, the cell had fast charging and discharging processes, which is desirable for applications requiring rapid energy storage and release.[7,45,46] The presence of an oxidation peak in the range of 0.7−1.0 V, originating from the electrode material, further supported the high specific capacitance of the cell, which showed the occurrence of electrochemical reactions associated with the charging process, suggesting efficient utilization of the electrode material for energy storage. The higher specific capacitance implies a larger amount of charge storage capability per unit mass of the electrode material. Additionally, during the reverse potential scan, the observation of a reduction peak at around 0.6−1 V suggested the occurrence of electrochemical reactions associated with the discharging process, demonstrating the release of the stored energy from the electrode material. Overall, the presence of these peaks and the behavior of the cyclic voltammograms indicated that the supercapacitor cell exhibits good rate capability, high specific capacitance, and efficient energy storage and release properties. While the parallelogram-like voltammogram represents the SWCNT and shows the electrostatic chargeability of the cell, the broad oxidation and reduction peaks are due to the **TT-TPA** in the structure exhibiting capacitive properties. Thienothiophene structures can provide a broad and repeatable range of oxidation and reduction reactions between 0.7 and 1.5 V.[47] Similarly, oxidation and reduction peaks were observed at 0.9 and 0.8 V, respectively (Figure 2a).

The specific capacitance values obtained from the cyclic voltammograms demonstrated the capacitance performance of the supercapacitor at different scan rates. As the scan rate increased, the specific capacitance slightly decreased, which was an expected trend at higher scan rates; the charging and discharging processes occurred more rapidly. This may limit

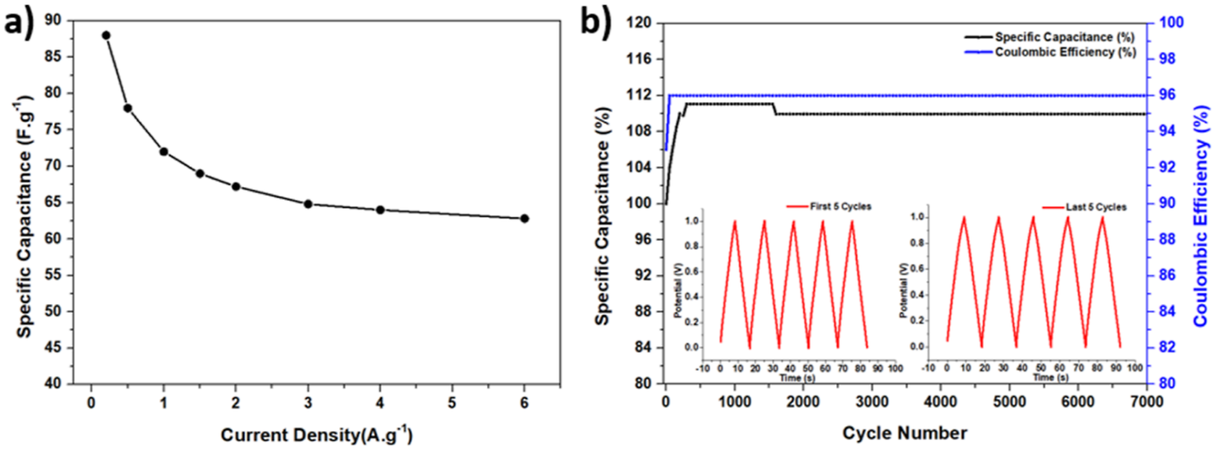

Figure 3. (a) Specific capacitances calculated from GCD plots at various current densities (0.1, 0.25, 0.5, 0.75, 1, 1.5, 2, and 3 A·g^{-1}) of the supercapacitor and (b) cycling stability of the supercapacitor cell.

the ability of the electrolyte ions to effectively access the electrode surface, resulting in a slightly reduced capacitance. The specific capacitance (C_{CV}) values, ranging from 83.2 F·g^{-1} at 5 mV·s^{-1} to 67.5 F·g^{-1} at 200 mV·s^{-1}, demonstrated the ability of the supercapacitor to store a significant amount of charge per unit mass of the electrode material (Figure 2b). Thus, **TT-TPA-SWCNT**, as an electrode, exhibited a high capacitance performance. Although there is a slight decrease in specific capacitance with the increasing scan rate, the overall capacitance values remained relatively high across the entire range, suggesting that the supercapacitor has good capacitance retention, even at higher scan rates. This is beneficial for applications requiring rapid energy storage and release. Thus, the obtained specific capacitance values indicated that the supercapacitor displaces an excellent capacitance performance with the ability to store a substantial amount of charge per unit mass of the electrode material, even at higher scan rates.

The Nyquist plot obtained from the experimental data exhibited a characteristic semicircle and a straight line (Figure 2c). The semicircle represents the charge transfer processes occurring at the electrode−electrolyte interface, while the straight line corresponds to the solution resistance and electrical connections within the supercapacitor cell. This plot provides valuable information about the impedance behavior of the system and allows for the determination of important resistance parameters. The resistance values were calculated by considering an equivalent circuit (Figure 2c). The resistances obtained from the Nyquist plot analysis are as follows: R_s, representing the solution resistance and electrical connections within the cell, was found to be 3.739 Ω, and $R_{ct}{}^{-1}$, associated with the charge transfer processes at the free-standing electrode, was determined to be 2.502 Ω. In the low-frequency region, almost 90°, a planar line was obtained. This represents an ideal capacitance characteristic for an active supercapacitor material.[48] These resistance values contribute to our understanding of the electrical behavior and performance of a supercapacitor system. The measurements were supported by galvanostatic charge−discharge tests. Low ohmic and charge transfer resistances enabled the material to reveal its capacitive nature.

Investigation of the charge and discharge curves displayed typical characteristics of a double-layer capacitor, confirming the capacitive behavior of the supercapacitor (Figure 2d). This observation reinforces an efficient utilization of the electric double-layer for energy storage and discharge. The GCD plots showed that both charge and discharge processes exhibited bending, which could be attributed to the faradaic reactions, identified in the cyclic voltammograms. Moreover, the bending indicated the involvement of redox reactions during the charging and discharging processes. An important aspect of the GCD analysis is nearly equal charge and discharge times, suggesting a high Coulombic efficiency of the supercapacitor cell. The balanced charge and discharge times is an indication of minimal energy losses and efficient energy transfer, resulting in a high overall Coulombic efficiency.

The specific capacitances obtained at different current densities provided insights into the capacitive performance of the supercapacitor. They were found to be 88, 78, 72, 69, 67.2, 64.8, 64, and 62.8 F·g^{-1} for the respective current densities of 0.2, 0.5, 1, 1.5, 2, 3, 4, and 6 A·g^{-1} (Figure 3a), indicating that the supercapacitor had a high capacitance and good rate capability. The GCD plots yielded energy densities of 3.05, 2.7, 2.5, 2.39, 2.33, 2.25, 2.22, and 2.18 W h·kg^{-1} at current densities of 0.2, 0.5, 1, 1.5, 2, 3, 4, and 6 A·g^{-1}, respectively. Furthermore, the power density of the supercapacitor ranged from 100 to 3000 W·kg^{-1}, demonstrating the rate at which the stored energy is delivered during discharge. These energy and power density values highlighted excellent performance of the supercapacitor in terms of its energy storage and delivery capabilities. The high energy densities show that the supercapacitor stores a substantial amount of energy per unit mass, making it suitable for applications requiring long-term energy storage. Additionally, the wide power density range demonstrated the versatility of the supercapacitor in delivering energy quickly; this is an advantage for applications requiring quick bursts of power.

The cycling stability of the free-standing electrode material in a two-electrode system was evaluated at a constant current density of 1 A·g^{-1} over 7000 cycles (Figure 3b). During the initial cycles, the specific capacitance gradually increased, indicating the activation and optimization of the electrode material. After approximately 100 cycles, the specific capacitance reached a stable plateau, demonstrating an enhanced electrode performance and improved charge storage capacity, which was attributed to the electrode accepting ions present in the operational environment. As the penetration of ions into an electrode increases, the electrode/electrolyte interface limitation temporarily decreases, leading to an

https://doi.org/10.1021/acsaem.3c02737
ACS Appl. Energy Mater. 2024, 7, 1488−1494

increase in specific capacitance.[49,50] Through the application of an electric current in the charging process, **TT-TPA** may accept SWCNT present in the environment as the substrate, resulting in oligomerization or polymerization on the surface. This remarkable phenomenon offers potential benefits such as reduced interface resistance between different electrode compositions within the structure and an overall enhancement in electrode conductivity. Moreover, after the charge−discharge cycling tests, the surface morphology of the **TT-TPA-SWCNT** electrode was re-examined using SEM analysis (Figure 4a,b) at different magnifications. The SEM pictures

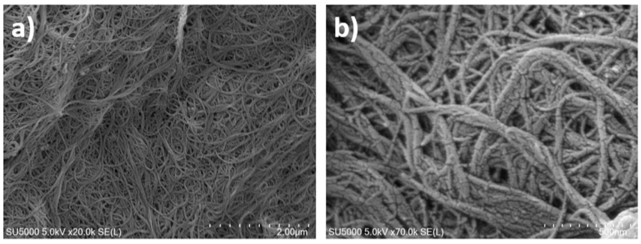

Figure 4. SEM images of the **TT-TPA-SWCNT** electrode after the cycling charge−discharge test at different magnifications (a) 2 μm and (b) 500 nm.

demonstrated similar interconnected and tangled bundles with the pristine **TT-TPA-SWCNT** on the electrode morphology (Figure 2b). On the other hand, formation of some cracks after the cycling were observed (Figure 4b), which possibly allowed the ions to penetrate into the electrode surface, causing an increase in certain amount of specific capacity, i.e., increase of specific capacitance after 500 cycles.[49,50] In the subsequent processes, no significant change in specific capacitance was observed, indicating that, despite the cracks, the electrode had no degradation, and SWCNT had a good adhesion with **TT-TPA**. This clearly shows that the **TT-TPA-SWCNT** hybrid material has very good cyclic stability.

Remarkably, the stable specific capacitance was maintained for around 1400 cycles, showcasing the excellent stability of the electrode material and sustained performance over a significant number of charge−discharge cycles. Moreover, the electrode exhibited exceptional cycling stability with approximately 110% capacity retention up to 7000 cycles. This signifies the remarkable ability of the free-standing electrode to retain its charge storage capacity, further emphasizing its suitability for long-term and reliable energy storage applications. Regarding all free-standing supercapacitor electrode comparisons, the performance of **TT-TPA-SWCNT** outperformed and competed with many hybrid SWCNT-based materials available in the literature.[13,51−54]

■ CONCLUSIONS

In conclusion, we present, for the first time, the use of TT and SWCNT-based hybrid materials, **TT-TPA-SWCNT**, as free-standing supercapacitors in high performance. The hybrid **TT-TPA-SWCNT**, obtained by noncovalent modification of SWCNT with electron-rich **TT-TPA** through directly attaching onto the SWCNT surface, was made clear by interconnected and tangled bundles of SEM, roughness from the cross-section of the 3D AFM, and obvious adsorption of Au nanoparticles on SWCNT of TEM analyses. The **TT-TPA-SWCNT** supercapacitor displayed a high specific capacitance of 83.2 $F \cdot g^{-1}$ at 5 $mV \cdot s^{-1}$, a maximum power density of 3000 $W \cdot kg^{-1}$, and an excellent retention capacity of 110% up to 7000 charge/discharge cycling stability. Considering these remarkable achievements, we believe the **TT-TPA-SWCNT** supercapacitor has great potential for practically portable and wearable electronic applications for clean and renewable energy-storage protocols.

■ ASSOCIATED CONTENT

Supporting Information

The Supporting Information is available free of charge at https://pubs.acs.org/doi/10.1021/acsaem.3c02737.

Raman analyses and synthetic procedure of the hybrid material (PDF)

■ AUTHOR INFORMATION

Corresponding Authors

Recep Isci − *Chemistry Department, Istanbul Technical University, Maslak, Istanbul 34469, Turkey;* orcid.org/0000-0003-3086-4478; Email: isci@itu.edu.tr

Turan Ozturk − *Chemistry Department, Istanbul Technical University, Maslak, Istanbul 34469, Turkey; TUBITAK UME, Chemistry Group Laboratories, Gebze, Kocaeli 41470, Turkey;* orcid.org/0000-0003-3777-5320; Email: ozturktur@itu.edu.tr

Authors

Koray Bahadir Donmez − *Sabanci University Nanotechnology Research and Application Center (SUNUM), Istanbul 34956, Turkey*

Nilgun Karatepe − *Energy Institute, Renewable Energy Division, Istanbul Technical University, Istanbul 34469, Turkey*

Complete contact information is available at: https://pubs.acs.org/10.1021/acsaem.3c02737

Notes

The authors declare no competing financial interest.

■ ACKNOWLEDGMENTS

We thank Istanbul Technical University (ITU), TGA-2023-45124 numbered ITU BAP Project, 122Z568 numbered TUBITAK project and Unsped Global Lojistik, Turkey, for financial support and Prof. Mehmet S. Eroglu of Marmara University for SEM measurements.

■ REFERENCES

(1) Liu, D.; Liu, J.; Wang, Q.; Du, P.; Wei, W.; Liu, P. PANI coated microporous graphene fiber capable of subjecting to external mechanical deformation for high performance flexible supercapacitors. *Carbon* **2019**, *143*, 147−153.

(2) Zhou, G.; Xu, L.; Hu, G.; Mai, Li.; Cui, Y. Nanowires for Electrochemical Energy Storage. *Chem. Rev.* **2019**, *119* (20), 11042−11109.

(3) Li, R.; Yang, Y.; Wu, D.; Li, K.; Qin, Y.; Tao, Y.; Kong, Y. Covalent functionalization of reduced graphene oxide aerogels with polyaniline for high performance supercapacitors. *Chem. Commun.* **2019**, *55*, 1738−1741.

(4) Lei, Z.; Shi, F.; Lu, L. Incorporation of MnO_2-Coated Carbon Nanotubes between Graphene Sheets as Supercapacitor Electrode. *ACS Appl. Mater. Interfaces* **2012**, *4* (2), 1058−1064.

(5) Czepa, W.; Witomska, S.; Ciesielski, A.; Samori, P. P. Reduced graphene oxide−silsesquioxane hybrid as a novel supercapacitor electrode. *Nanoscale* **2020**, *12*, 18733−18741.

(6) Lu, X.; Yu, M.; Wang, G.; Tong, Y.; Li, Y. Flexible solid-state supercapacitors: design, fabrication and applications. *Energy Environ. Sci.* **2014**, *7*, 2160−2181.
(7) Blackburn, J. L. Semiconducting Single-Walled Carbon Nanotubes in Solar Energy Harvesting. *ACS Energy Lett.* **2017**, *2* (7), 1598−1613.
(8) Wang, Q.; Chen, Y.; Jiang, X.; Qiao, X.; Wang, Y.; Zhao, H.; Pu, B.; Yang, W. Self-assembly defect-regulating superstructured carbon. *Energy Storage Mater.* **2022**, *48*, 164−171.
(9) Wang, Q.; Qu, Y.; Bai, J.; Chen, Z.; Luo, Q.; Li, H.; Li, J.; Yang, W. High-yield ramie derived carbon toward high-performance supercapacitors. *Nano Energy* **2024**, *120*, 109147.
(10) Wang, Q.; Jiang, X.; Tong, Q.; Li, H.; Li, J.; Yang, W. Continuously Interconnected N-Doped Porous Carbon for High-Performance Lithium-Ion Capacitors. *Nano Energy Adv.* **2022**, *2*, 303−315.
(11) Chen, R. J.; Zhang, Y.; Wang, D.; Dai, H. Noncovalent Sidewall Functionalization of Single-Walled Carbon Nanotubes for Protein Immobilization. *J. Am. Chem. Soc.* **2001**, *123* (16), 3838−3839.
(12) Niu, Z.; Zhou, W.; Chen, J.; Feng, G.; Li, H.; Ma, W.; Li, J.; Dong, H.; Ren, Y.; Zhao, D.; Xie, S. Compact-designed supercapacitors using free-standing single-walled carbon nanotube films. *Energy Environ. Sci.* **2011**, *4*, 1440−1446.
(13) Wu, G.; Tan, P.; Wang, D.; Li, Z.; Peng, L.; Hu, Y.; Wang, C.; Zhu, W.; Chen, S.; Chen, W. High-performance Supercapacitors Based on Electrochemical-induced Vertical-aligned Carbon Nanotubes and Polyaniline Nanocomposite Electrodes. *Sci. Rep.* **2017**, *7*, 43676.
(14) Li, Z.; Tozer, T.; Alisaraie, L. Molecular Dynamics Studies for Optimization of Noncovalent Loading of Vinblastine on Single-Walled Carbon Nanotube. *J. Phys. Chem. C* **2016**, *120* (7), 4061−4070.
(15) Rashidi, A. M.; Nouralishahi, A.; Khodadadi, A. A.; Mortazavi, Y.; Karimi, A.; Kashefi, K. Modification of single wall carbon nanotubes (SWNT) for hydrogen storage. *Int. J. Hydrogen Energy* **2010**, *35* (17), 9489−9495.
(16) Georgakilas, V.; Tiwari, J. N.; Kemp, K. C.; Perman, J. A.; Bourlinos, A. B.; Kim, K. S.; Zboril, R. Noncovalent Functionalization of Graphene and Graphene Oxide for Energy Materials, Biosensing, Catalytic, and Biomedical Applications. *Chem. Rev.* **2016**, *116* (9), 5464−5519.
(17) Ren, X.; Zhao, Y.; Yang, B.; Wang, X.; Wei, Y.; Tao, L. One-pot polymer modification of carbon nanotubes through mercaptoacetic acid locking imine reaction and $\pi-\pi$ stacking. *RSC Adv.* **2015**, *5* (67), 54133−54137.
(18) Norizan, M. N.; Moklis, M. H.; Ngah Demon, S. Z.; Halim, N. A.; Samsuri, A.; Mohamad, I. S.; Knight, V. F.; Abdullah, N. Carbon nanotubes: functionalisation and their application in chemical sensors. *RSC Adv.* **2020**, *10* (71), 43704−43732.
(19) Pan, H.; Li, J.; Feng, Y. Carbon Nanotubes for Supercapacitor. *Nanoscale Res. Lett.* **2010**, *5*, 654−668.
(20) Choi, E. Y.; Choi, L. W.; Kim, C. K. Noncovalent functionalization of multi-walled carbon nanotubes with hydroxyl group-containing pyrene derivatives for their composites with polycarbonate. *Carbon* **2015**, *95*, 91−99.
(21) Di Crescenzo, A.; Ettorre, V.; Fontana, A. Non-covalent and reversible functionalization of carbon nanotubes. *Beilstein J. Nanotechnol.* **2014**, *5*, 1675−1690.
(22) Isci, R.; Tekin, E.; Kaya, K.; Piravadili Mucur, S.; Gorkem, S. F.; Ozturk, T. Tetraphenylethylene substituted thienothiophene and dithienothiophene derivatives: synthesis, optical properties and OLED applications. *J. Mater. Chem. C* **2020**, *8*, 7908−7915.
(23) Isci, R.; Tekin, E.; Mucur, S. P.; Ozturk, T. A Bifunctional Bulky Thienothiophene Derivative; Synthesis, Electronic-Optical Properties and OLED Applications. *ChemistrySelect* **2020**, *5*, 13091−13098.
(24) Turkoglu, G.; Cinar, M. E.; Ozturk, T. Synthesis and Photophysical and Anion-Sensing Properties of Triarylborane-Substituted Cross-Conjugated and Conjugated Thienothiophenes. *Eur. J. Org Chem.* **2017**, *2017*, 4552−4561.
(25) Isci, R.; Wan, L.; Topal, S.; Gunturkun, D.; Campbell, A. J.; Ozturk, T. Solution-Processable Donor−π−Acceptor Type Thieno[3,2-*b*]Thiophene Derivatives; Synthesis, Photophysical Properties and Applications. *J. Mater. Chem. C* **2022**, *10* (29), 10719−10727.
(26) Amna, B.; Isci, R.; Siddiqi, H. M.; Majewski, L. A.; Faraji, S.; Ozturk, T. High-Performance, Low-Voltage Organic Field-Effect Transistors Using Thieno[3,2-*b*]thiophene and Benzothiadiazole Co-Polymers. *J. Mater. Chem. C* **2022**, *10*, 8254−8265.
(27) Isci, R.; Balkan, T.; Tafazoli, S.; Sütay, B.; Eroglu, M. S.; Ozturk, T. Thienothiophene and Triphenylbenzene Based Electroactive Conjugated Porous Polymer for Oxygen Reduction Reaction (ORR). *ACS Appl. Energy Mater.* **2022**, *5* (11), 13284−13292.
(28) Gunturkun, D.; Isci, R.; Sütay, B.; Majewski, L. A.; Faraji, S.; Ozturk, T. Copolymers of 3-Arylthieno[3,2-*b*]thiophenes Bearing Different Substituents: Synthesis, Electronic, Optical, Sensor and Memory Properties. *Eur. Polym. J.* **2022**, *170*, 111167.
(29) Topal, S.; Isci, R.; Sezer, E.; Ozturk, T.; Ustamehmetoglu, B. Synthesis and electropolymerization of 3-arylthieno[3,2-*b*]thiophenes and triphenylamine based comonomers. *Electrochim. Acta* **2021**, *389*, 138688.
(30) Ozturk, S. E.; Isci, R.; Faraji, S.; Sütay, B.; Majewski, L. A.; Ozturk, T. Synthesis, Photophysical properties and OFET application of thienothiophene and benzothiadiazole based Donor-π-Acceptor-π (D-π-A-π) type conjugated polymers. *Eur. Polym. J.* **2023**, *191*, 112028.
(31) Isci, R.; Unal, M.; Yesil, T.; Ekici, A.; Sütay, B.; Zafer, C.; Ozturk, T. Thieno[3,2-*b*]thiophene and triphenylamine-based hole transport materials for perovskite solar cells. *Front. Mater.* **2023**, *10*, 174.
(32) Isci, R.; Rahimi Varzeghani, A.; Kaya, K.; Sütay, B.; Tekin, E.; Ozturk, T. Triphenylamine/Tetraphenylethylene Substituted 4-Thieno[3,2-*b*]thiophen-3-ylbenzonitriles: Synthesis, Photophysical-Electronic Properties, and Applications. *ACS Sustainable Chem. Eng.* **2022**, *10* (4), 1605−1615.
(33) Cinar, M. E.; Ozturk, T. Thienothiophenes, Dithienothiophenes, and Thienoacenes: Syntheses, Oligomers, Polymers, and Properties. *Chem. Rev.* **2015**, *115*, 3036−3140.
(34) Isci, R.; Ozturk, T. Thienothiophene-based organic light-emitting diode: synthesis, photophysical properties and application. *Beilstein J. Org. Chem.* **2023**, *19*, 1849−1857.
(35) İşçi, R.; Ozturk, T. A multifunctional thienothiophene member: 4-thieno [3,2-b] thiophen-3-ylbenzonitrile (4-CNPhTT). *Turk. J. Chem.* **2023**, *47* (5), 1239−1248.
(36) Isci, R.; Gencosman, E.; Yagci, Y.; Ozturk, T. Thienothiophene and biphenyl based conjugated porous polymer as a photocatalyst for visible light induced free radical and cationic polymerization. *J. Photochem. Photobiol., A* **2024**, *449*, 115427.
(37) Cao, X.-M.; Sun, Z.-J.; Zhao, S.-Y.; Wang, B.; Han, Z.-B. MOF-derived sponge-like hierarchical porous carbon for flexible all-solid-state supercapacitors. *Mater. Chem. Front.* **2018**, *2* (9), 1692−1699.
(38) Chen, X. Y.; Chen, C.; Zhang, Z. J.; Xie, D. H. Gelatin-derived nitrogen-doped porous carbon via a dual-template carbonization method for high performance supercapacitors. *J. Mater. Chem. A* **2013**, *1*, 10903−10911.
(39) Yu, J.; Fu, N.; Zhao, J.; Liu, R.; Li, F.; Du, Y.; Yang, Z. High Specific Capacitance Electrode Material for Supercapacitors Based on Resin-Derived Nitrogen-Doped Porous Carbons. *ACS Omega* **2019**, *4* (14), 15904−15911.
(40) Stoller, M. D.; Ruoff, R. S. Best practice methods for determining an electrode material's performance for ultracapacitors. *Energy Environ. Sci.* **2010**, *3*, 1294−1301.
(41) Suerkan, A.; Isci, R.; Ozturk, T.; Yagci, Y. Cationic and radical polymerization using a boron−thienothiophene−triphenylamine based D−π−A type photosensitizer under white LED irradiation. *Mol. Syst. Des. Eng.* **2023**, *8* (10), 1319−1326.
(42) Gunturkun, D.; Isci, R.; Faraji, S.; Sütay, B.; Majewski, L. A.; Ozturk, T. Synthesis and characterization of naphthalenediimide-

thienothiophene-conjugated polymers for OFET and OPT applications. *J. Mater. Chem. C* **2023**, *11* (38), 13129−13141.

(43) Isci, R.; Unal, M.; Kucukcakir, G.; Gurbuz, N. A.; Gorkem, S. F.; Ozturk, T. Triphenylamine/4,4′-Dimethoxytriphenylamine-Functionalized Thieno[3,2-*b*]thiophene Fluorophores with a High Quantum Efficiency: Synthesis and Photophysical Properties. *J. Phys. Chem. B* **2021**, *125*, 13309−13319.

(44) Isci, R.; Baysak, E.; Kesan, G.; Minofar, B.; Eroglu, M. S.; Duygulu, O.; Gorkem, S. F.; Ozturk, T. Noncovalent Modification of Single Wall Carbon Nanotubes (SWCNTs) by Thienothiophene Derivatives. *Nanoscale* **2022**, *14* (44), 16602−16610.

(45) Cheng, J.; Lu, Z.; Zhao, X.; Chen, X.; Liu, Y. Green needle coke-derived porous carbon for high-performance symmetric supercapacitor. *J. Power Sources* **2021**, *494*, 229770.

(46) Zhang, M.; Song, Y.; Li, W.; Huang, X.; Wang, C.; Song, T.; Hou, X.; Luan, S.; Wang, T.; Wang, T.; Wang, Q. CO_2 assisted synthesis of hierarchical porous carbon for supercapacitor electrode and dye adsorbent. *Inorg. Chem. Front.* **2019**, *6*, 1141−1151.

(47) Baghdouche, A. K.; Guergouri, M.; Bencharif, M.; Bencharif, L. Synthesis, characterization, and electropolymerization of fluorene-thiophene derivatives. *J. Mol. Struct.* **2022**, *1252*, 132091.

(48) Wang, Q.; Chen, Z.; Luo, Q.; Li, H.; Li, J.; Yang, W. Capillary Evaporation on High-Dense Conductive Ramie Carbon for Assisting Highly Volumetric-Performance Supercapacitors. *Small* **2023**, *19*, 2303349.

(49) Sirisinudomkit, P.; Senokos, E.; Rubio, N.; Shaffer, M. S. P. Reductive processing of single walled carbon nanotubes for high volumetric performance supercapacitors. *Mater. Adv.* **2021**, *2*, 1981−1992.

(50) Pan, C.; Gu, H.; Dong, L. Synthesis and electrochemical performance of polyaniline @MnO2/graphene ternary composites for electrochemical supercapacitors. *J. Power Sources* **2016**, *303*, 175−181.

(51) Xia, H.; Hong, C.; Li, B.; Zhao, B.; Lin, Z.; Zheng, M.; Savilov, S. V.; Aldoshin, S. M. Facile Synthesis of Hematite Quantum-Dot/Functionalized Graphene-Sheet Composites as Advanced Anode Materials for Asymmetric Supercapacitors. *Adv. Funct. Mater.* **2015**, *25*, 627−635.

(52) Campbell, P. G.; Merrill, M. D.; Wood, B. C.; Montalvo, E.; Worsley, M. A.; Baumann, T. F.; Biener, J. Battery/supercapacitor hybrid via non-covalent functionalization of graphene macro-assemblies. *J. Mater. Chem. A* **2014**, *2* (42), 17764−17770.

(53) Yoon, J.; Lee, J.; Hur, J. Stretchable Supercapacitors Based on Carbon Nanotubes-Deposited Rubber Polymer Nanofibers Electrodes with High Tolerance against Strain. *Nanomaterials* **2018**, *8* (7), 541.

(54) Zhang, Y.; Zhang, H.; Jiang, F.; Zhou, W.; Wang, R.; Xu, J.; Duan, X.; Wu, Y.; Ding, Y. Electrochemical assembly of homogenized poly(3,4-ethylenedioxythiophene methanol)/SWCNT nanonetworks and their high performances for supercapacitor electrodes. *Ionics* **2020**, *26*, 3631−3642.

https://doi.org/10.1021/acsaem.3c02737
ACS Appl. Energy Mater. 2024, 7, 1488−1494